Analysis and Simplification of the GTF Model of the Belousov–Zhabotinsky Reaction

Tamás Turányi

Central Research Institute for Chemistry of the Hungarian Academy of Sciences, H-1525 Budapest, P.O. Box 17, Hungary, and School of Chemistry, The University of Leeds, Leeds LS2 9JT, United Kingdom

László Györgyi*

Department of Inorganic and Analytical Chemistry, Eötvös University, H-1518 Budapest-112, P.O. Box 32, Hungary, and Department of Chemistry, Brandeis University, Waltham, Massachusetts 02254

Richard J. Field

Department of Chemistry, University of Montana, Missoula, Montana 59812

Received: November 16, 1992

An 80-reaction, 26-species mechanistic model of the oscillatory Belousov–Zhabotinsky (BZ) reaction recently introduced by Györgyi, Turányi and Field (GTF model) is analyzed in this work. Major reaction interactions within the large mechanism are revealed, and by reaction rate sensitivity analysis redundant species and reactions are identified. Removal of these results in a 42-reaction, 22-species mechanism that quantitatively agrees with the original model in three test simulations. This mechanism was further simplified to 3-variable ($HBrO_2$, Br^-, Ce(IV)) skeleton models that are oscillatory under the conditions where the transient oscillations appear in the batch simulations. Two such models are put forward that oscillate without any change in the original parameter values. These skeleton models are contrasted with the Oregonator model and proved to be better description of the experimental system. It is of particular interest that these simple models do not contain any adjustable parameters. The 42-reaction mechanism is suggested as a starting point for further modeling studies with the BZ reaction. This model still contains both negative feedbacks suggested for this system, the bromide-control and the organic radical control. In the skeletons only the inhibition by bromide ions is necessary for the oscillations to occur. The simplification process reveals that the radical transfer process between malonyl radical and bromomalonic acid is of great importance in this mechanism. Recent experimental study by Försterling and Stuk finds this reaction to be unimportant in the BZ chemistry. We propose the addition of the hydrolysis of bromomalonyl radical to the GTF model to deal with the problem and with that provide an alternative interpretation for the above experiments.

Introduction

The Belousov[1]–Zhabotinsky[2] (BZ) reaction is a textbook example of nonlinear dynamics in chemical systems. It exhibits sustained oscillations in closed system, bistability, birhythmicity, complex limit cycles and strange attractors in well-stirred open system, and traveling waves in spatially distributed systems. The most studied, "classical" BZ system consists of bromate ions, malonic acid ($CH_2(COOH)_2$) and Ce(III) or Ce(IV) as a catalyst in approximately 1 M sulfuric acid solution. The overall chemical reaction is the cerium catalyzed oxidation and bromination of malonic acid by acidic bromate. Depending on the initial concentrations (or the flow concentrations in an open system) the concentration of the intermediates of the system may oscillate during this process. The first quantitative account for the chemistry occurring during oscillations in this system is due to Field, Körös and Noyes[3] and is referred to as the FKN mechanism. Although the inorganic reaction set of the FKN mechanism is generally accepted, the processes containing organic intermediates are the subject of active research. In an attempt to summarize the current status of this research and to suggest explanations to some open mechanistical problems we introduced[4] a mechanism of the BZ reaction that contains 80 reaction and 26 components of variable concentration. This mechanism is often referred to as GTF mechanism and is shown in Table I. It was successful at quantitatively or semiquantitatively reproducing several experiments performed with the BZ reaction and its subsets mostly in oxygen free environment.

The oscillations observed in simulations can be interpreted by identifying major feedback loops[3,5] in the mechanism in Table I as follows. Reactions 9–14 are a sequence that is autocatalytic in $HBrO_2$ and it oxidizes Ce(III) to Ce(IV). This $HBrO_2$ autocatalysis is the major positive feedback of the mechanism. This sequence of reactions itself would result in a high-[$HBrO_2$], high-[Ce(IV)], oxidized steady state that is also characterized by low [Br^-] because of reaction 3. Under conditions appropriate for oscillations the oxidized state can not gain permanent dominance since with some delay the Ce(IV) produced in reaction 13 produces an intermediate that removes $HBrO_2$, thus inhibiting the autocatalytic reaction. This is a delayed negative feedback, and the assumption of the FKN mechanism was that Ce(IV) deliberates Br^- from the brominated organic material (e.g. bromomalonic acid, BrMA) and this removes $HBrO_2$ in reaction 3. When the autocatalysis is stopped (since the rate of reaction 3 is much larger than that of reaction 9) [Br^-] becomes high, and the system switches to a high-[Br^-], low-[$HBrO_2$], low-[Ce(IV)], reduced state. The reduced state prevails until enough Br^- is consumed in reaction 5 to decrease its concentration to a level where reaction 9 is faster than reaction 3, and the autocatalytic process may start again. Because of this inhibiting role of bromide ion the BZ oscillations were termed "bromide-controlled". There have been some new developments in the details of this negative feedback since the FKN mechanism had been introduced. In a series of papers Försterling, Noszticzius and co-workers argued[6-8] that malonly radical (resulting from the oxidation of malonic acid, MA, by Ce(IV)) reacts at a diffusion-controlled rate in reaction 46 with $BrO_2^\bullet$, an intermediate of the $HBrO_2$ autocatalysis. If the product of this reaction is not $HBrO_2$ then this process is another negative feedback analogously with what is described for bromide ion above. In this "radical-controlled" mechanism the malonyl radicals stop the autocatalysis and keep the concentration of $HBrO_2$ low until they are consumed in reaction 41. It is still debated how much role the radical-control

0022-3654/93/2097-1931$04.00/0

TABLE I: Mechanistic Model[a] of the Belousov–Zhabotinsky Reaction ([H_2O] = 55 M Included in the Rate Constants)

	1. Inorganic Subset				
(1)	$HOBr + Br^- + H^+ \rightarrow Br_2 + H_2O$	2.3E+9 M^{-2} s^{-1}	(8)	$BrO_3^- + HOBr + H^+ \rightarrow 2HBrO_2$	7.5E-9 M^{-2} s^{-1}
(2)	$Br_2 + H_2O \rightarrow HOBr + Br^- + H^+$	2.0 s^{-1}	(9)	$BrO_3^- + HBrO_2 + H^+ \rightarrow Br_2O_4 + H_2O$	33.0 M^{-2} s^{-1}
(3)	$Br^- + HBrO_2 + H^+ \rightarrow 2HOBr$	2.0E+6 M^{-2} s^{-1}	(10)	$Br_2O_4 + H_2O \rightarrow BrO_3^- + HBrO_2 + H^+$	2200 s^{-1}
(4)	$2HOBr \rightarrow Br^- + HBrO_2 + H^+$	2.0E-5 M^{-1} s^{-1}	(11)	$Br_2O_4 \rightarrow 2BrO_2^\bullet$	7.4E+4 s^{-1}
(5)	$Br^- + BrO_3^- + 2H^+ \rightarrow HOBr + HBrO_2$	2.0 M^{-3} s^{-1}	(12)	$2BrO_2^\bullet \rightarrow Br_2O_4$	1.4E+9 M^{-1} s^{-1}
(6)	$HOBr + HBrO_2 \rightarrow Br^- + BrO_3^- + 2H^+$	3.3 M^{-1} s^{-1}	(13)	$Ce^{3+} + BrO_2^\bullet + H^+ \rightarrow HBrO_2 + Ce^{4+}$	6.2E+4 M^{-2} s^{-1}
(7)	$2HBrO_2 \rightarrow BrO_3^- + HOBr + H^+$	3.0E+3 M^{-1} s^{-1}	(14)	$HBrO_2 + Ce^{4+} \rightarrow Ce^{3+} + BrO_2^\bullet + H^+$	7.0E+3 M^{-1} s^{-1}
	2. Reactions Involving Organic Species				
	(a) Reactions Not Consuming or Producing Radicals				
(15)	$MA \rightarrow ENOL$	3.0E-3 s^{-1}	(20)	$TTA + HOBr \rightarrow BrTTA + H_2O$	5.0 M^{-1} s^{-1}
(16)	$ENOL \rightarrow MA$	200.0 s^{-1}	(21)	$BrO_2MA + H_2O \rightarrow HBrO_2 + TTA$	1.0 s^{-1}
(17)	$ENOL + Br_2 \rightarrow BrMA + Br^- + H^+$	1.91E+6 M^{-1} s^{-1}	(22)	$BrO_2MA \rightarrow HOBr + MOA$	1.0 s^{-1}
(18)	$MA + HOBr \rightarrow BrMA + H_2O$	8.2 M^{-1} s^{-1}	(23)	$BrO_2TTA \rightarrow HBrO_2 + MOA$	1.0 s^{-1}
(19)	$BrMA + HOBr \rightarrow Br_2MA + H_2O$	0.1 M^{-1} s^{-1}	(24)	$BrTTA \rightarrow Br^- + MOA + H^+$	1.0 s^{-1}
	(b) Reactions Producing Radicals				
(25)	$Ce^{4+} + BrMA \rightarrow Ce^{3+} + BrMA^\bullet + H^+$	0.09 M^{-1} s^{-1}	(30)	$HOBr + OA \rightarrow Br^\bullet + {}^\bullet COOH + CO_2 + H_2O$	140.0 M^{-1} s^{-1}
(26)	$Ce^{4+} + MA \rightarrow Ce^{3+} + MA^\bullet + H^+$	0.23 M^{-1} s^{-1}	(31)	$Ce^{4+} + OA \rightarrow Ce^{3+} + {}^\bullet COOH + CO_2 + H^+$	10.0 M^{-1} s^{-1}
(27)	$Ce^{4+} + TTA \rightarrow Ce^{3+} + TTA^\bullet + H^+$	0.66 M^{-1} s^{-1}	(32)	$BrO_3^- + OA + H^+ \rightarrow BrO_2^\bullet + {}^\bullet COOH + CO_2 + H_2O$	1.6E-5 M^{-2} s^{-1}
(28)	$HOBr + MOA \rightarrow Br^\bullet + OA + {}^\bullet COOH$	140.0 M^{-1} s^{-1}			
(29)	$Ce^{4+} + MOA + H_2O \rightarrow Ce^{3+} + OA + {}^\bullet COOH + H^+$	10.0 M^{-1} s^{-1}			
	(c) Reactions Consuming Radicals				
(33)	$2Br^\bullet \rightarrow Br_2$	1.0E+8 M^{-1} s^{-1}	(44)	$MA^\bullet + Br^\bullet \rightarrow BrMA$	1.0E+9 M^{-1} s^{-1}
(34)	$Br^\bullet + BrMA^\bullet \rightarrow Br_2MA$	1.0E+9 M^{-1} s^{-1}	(45)	$MA^\bullet + Ce^{3+} + H^+ \rightarrow MA + Ce^{4+}$	1.7E+4 M^{-2} s^{-1}
(35)	$2BrMA^\bullet + H_2O \rightarrow BrMA + BrTTA$	1.0E+8 M^{-1} s^{-1}	(46)	$MA^\bullet + BrO_2^\bullet \rightarrow BrO_2\,MA$	5.0E+9 M^{-1} s^{-1}
(36)	$BrMA^\bullet + MA^\bullet + H_2O \rightarrow MA + BrTTA$	1.0E+9 M^{-1} s^{-1}	(47)	$2TTA^\bullet \rightarrow TTA + MOA$	1.0E+9 M^{-1} s^{-1}
(37)	$BrMA^\bullet + TTA^\bullet + H_2O \rightarrow TTA + BrTTA$	1.0E+9 M^{-1} s^{-1}	(48)	$TTA^\bullet + {}^\bullet COOH \rightarrow TTA + CO_2$	2.0E+9 M^{-1} s^{-1}
(38)	$BrMA^\bullet + Ce^{4+} + H_2O \rightarrow Ce^{3+} + BrTTA + H^+$	1.0E+7 M^{-1} s^{-1}	(49)	$TTA^\bullet + Br^\bullet \rightarrow BrTTA$	1.0E+9 M^{-1} s^{-1}
			(50)	$TTA^\bullet + Ce^{3+} + H^+ \rightarrow TTA + Ce^{4+}$	1.7E+4 M^{-2} s^{-1}
(39)	$BrMA^\bullet + BrO_2^\bullet + H_2O \rightarrow HBrO_2 + BrTTA$	5.0E+9 M^{-1} s^{-1}	(51)	$TTA^\bullet + BrO_2^\bullet \rightarrow BrO_2TTA$	5.0E+9 M^{-1} s^{-1}
(40)	$BrMA^\bullet + {}^\bullet COOH \rightarrow BrMA + CO_2$	5.0E+8 M^{-1} s^{-1}	(52)	$2{}^\bullet COOH \rightarrow OA$	1.2E+9 M^{-1} s^{-1}
(41)	$2MA^\bullet + H_2O \rightarrow MA + TTA$	3.2E+9 M^{-1} s^{-1}	(53)	$^\bullet COOH + Ce^{4+} \rightarrow Ce^{3+} + CO_2 + H^+$	1.0E+7 M^{-1} s^{-1}
(42)	$MA^\bullet + TTA^\bullet + H_2O \rightarrow 2TTA$	1.0E+9 M^{-1} s^{-1}	(54)	$^\bullet COOH + Br^\bullet \rightarrow Br^- + CO_2 + H^+$	1.0E+9 M^{-1} s^{-1}
(43)	$MA^\bullet + {}^\bullet COOH \rightarrow MA + CO_2$	2.0E+9 M^{-1} s^{-1}	(55)	$^\bullet COOH + BrO_2^\bullet \rightarrow HBrO_2 + CO_2$	5.0E+9 M^{-1} s^{-1}
	(d) Reactions Preserving Radicals				
(56)	$MA^\bullet + Br_2 \rightarrow BrMA + Br^\bullet$	1.5E+8 M^{-1} s^{-1}	(69)	$BrMA^\bullet + HOBr \rightarrow BrTTA + Br^\bullet$	1.0E+5 M^{-1} s^{-1}
(57)	$MA^\bullet + HOBr \rightarrow TTA + Br^\bullet$	1.0E+7 M^{-1} s^{-1}	(70)	$BrMA^\bullet + BrO_3^- + H^+ \rightarrow BrO_2^\bullet + BrTTA$	40.0 M^{-2} s^{-1}
(58)	$MA^\bullet + BrO_3^- + H^+ \rightarrow TTA + BrO_2^\bullet$	40.0 M^{-2} s^{-1}	(71)	$^\bullet COOH + BrMA \rightarrow Br^- + MA^\bullet + CO_2 + H^+$	1.0E+7 M^{-1} s^{-1}
(59)	$MA^\bullet + TTA \rightarrow MA + TTA^\bullet$	1.0E+5 M^{-1} s^{-1}	(72)	$^\bullet COOH + Br_2 \rightarrow Br^- + Br^\bullet + CO_2 + H^+$	1.5E+8 M^{-1} s^{-1}
(60)	$TTA^\bullet + MA \rightarrow TTA + MA^\bullet$	1.0E+5 M^{-1} s^{-1}	(73)	$^\bullet COOH + HOBr \rightarrow Br^\bullet + CO_2 + H_2O$	2.0E+7 M^{-1} s^{-1}
(61)	$MA^\bullet + BrMA \rightarrow MA + BrMA^\bullet$	1.0E+5 M^{-1} s^{-1}	(74)	$^\bullet COOH + BrO_3^- + H^+ \rightarrow BrO_2^\bullet + CO_2 + H_2O$	2.1E+3 M^{-2} s^{-1}
(62)	$BrMA^\bullet + MA \rightarrow BrMA + MA^\bullet$	5.0E+2 M^{-1} s^{-1}			
(63)	$TTA^\bullet + BrMA \rightarrow TTA + BrMA^\bullet$	2.0E+5 M^{-1} s^{-1}	(75)	$Br^\bullet + MA \rightarrow Br^- + MA^\bullet + H^+$	1.0E+5 M^{-1} s^{-1}
(64)	$BrMA^\bullet + TTA \rightarrow BrMA + TTA^\bullet$	5.0E+3 M^{-1} s^{-1}	(76)	$Br^\bullet + TTA \rightarrow Br^- + TTA^\bullet + H^+$	1.0E+6 M^{-1} s^{-1}
(65)	$TTA^\bullet + Br_2 \rightarrow BrTTA + Br^\bullet$	1.0E+8 M^{-1} s^{-1}	(77)	$Br^\bullet + BrMA \rightarrow Br^- + BrMA^\bullet + H^+$	5.0E+6 M^{-1} s^{-1}
(66)	$TTA^\bullet + HOBr \rightarrow MOA + Br^\bullet + H_2O$	1.0E+7 M^{-1} s^{-1}	(78)	$Br^\bullet + MOA + H_2O \rightarrow Br^- + OA + {}^\bullet COOH + H^+$	2.0E+3 M^{-1} s^{-1}
(67)	$TTA^\bullet + BrO_3^- + H^+ \rightarrow MOA + BrO_2^\bullet + H_2O$	40.0 M^{-2} s^{-1}			
			(79)	$Br^\bullet + OA \rightarrow Br^- + {}^\bullet COOH + CO_2 + H^+$	2.0E+3 M^{-1} s^{-1}
(68)	$BrMA^\bullet + Br_2 \rightarrow Br_2MA + Br^\bullet$	1.0E+6 M^{-1} s^{-1}	(80)	$BrO_2^\bullet + OA \rightarrow HBrO_2 + {}^\bullet COOH + CO_2$	1.0E+2 M^{-1} s^{-1}

[a] Abbreviations: MA ≡ $CH_2(COOH)_2$; $MA^\bullet$ ≡ $^\bullet CH(COOH)_2$; BrMA ≡ $BrCH(COOH)_2$; TTA ≡ $HCOH(COOH)_2$; Br_2MA ≡ $CBr_2(COOH)_2$; $BrMA^\bullet$ ≡ $^\bullet CBr(COOH)_2$; $TTA^\bullet$ ≡ $^\bullet COH(COOH)_2$; BrTTA ≡ $BrCOH(COOH)_2$; ENOL ≡ $(HOOC)CH{=}C(OH)_2$; MOA ≡ $CO(COOH)_2$; BrO_2MA ≡ $OBrOCH(COOH)_2$; OA ≡ $(COOH)_2$; BrO_2TTA ≡ $OBrOCOH(COOH)_2$.

has in the classical BZ reaction and we address this issue both in our previous[4] and in this work at least on the level of model studies.

Since its publication the GTF model has been tested[9] by modeling phase shifts of the oscillations caused by the addition of $HBrO_2$, and some of its reactions have been experimentally studied.[10,11] While in the first case the model performed adequately, the radical transfer reaction between $MA^\bullet$ and BrMA, an important process of the model, was claimed[10] to have a negligible rate, though this indirect conclusion can be argued (see Discussion and Appendix).

In this work we attempt to identify the minimal set of reactions that still quantitatively reproduces the behavior of the original GTF mechanism. There are two main reasons for doing this: The first is that if modifications are necessary it is easier to deal with a smaller set of reactions. Second, there is a number of reactions and rate constants in the model that were suggested by analogy to other reactions. An experimental verification of these assumptions is necessary, but it is helpful if the experiments can concentrate on processes that are important in generating the observed behavior of the model. We also attempt to find the skeleton model that can describe oscillations in the GTF mechanism. Until now the three-variable Oregonator model[12] has been the main testing ground for the exotic phenomena exhibited by the BZ system. An exception to this is the chemical chaos and complex oscillations that the Oregonator is not able to reproduce, and alternative small models have been suggested[13,14] recently. Regardless of the recent criticism,[10] the GTF model is still the most complete representation of the chemistry of this complex system. It has 66 reactions that contain organic reactant. In the Oregonator[12] the role of these reactions is played by a single step:

$$2Ce(IV) \rightarrow f Br^- \qquad (O5)$$

that was not assumed by systematic simplification of a more complete mechanism, but by using chemical intuition based on the FKN mechanism. Thus it is of interest to extract the essence

of the 66-reaction organic subset. The same can be done with the inorganic subset (reactions 1–14) so that a minimal set of reactions is identified that reproduce the oscillations in this system and which can be contrasted with the original Oregonator model.

In this work we present a 42-reaction subset of the original GTF model that reproduces accurately the behavior of the 80-reaction mechanism in certain test simulations and we suggest that it could replace the GTF model for most BZ simulation purposes. Further simplification leads to 3-variable schemes that exhibit limit-cycle oscillations under the experimental circumstances and match experiments better than the Oregonator model.

Analysis and Reduction of the Model

Methodology of Model Reduction. The analysis and reduction of the GTF mechanism were performed by using the reaction rate sensitivity method of Turányi.[15,16] A short summary of this procedure follows in the next paragraphs, but for a detailed description of this and other sensitivity methods we refer to the literature.[17]

Sensitivity calculations,[17] in general, provide us with information on the importance of a single reaction in determining the concentration (or its time derivative) of a single species of the mechanism. In order to assess the importance of reactions in determining the observed behavior of the model the effect of individual reactions on several species has to be simultaneously investigated. This can be done by studying an appropriate objective function that combines the information about the sensitivity of chemical components of interest. In the reaction rate sensitivity calculations the matrix of log-normalized partial derivatives of the right-hand-sides of the set of differential equations resulting from the chemical model with respect to the rate constants ($\mathbf{F} = \{\partial \ln f_i/\partial \ln k_j\}$) is analyzed at particular times of a simulation. The principal component analysis[15] (PCA) of F, i.e., determining the eigenvalues and eigenvectors of $\mathbf{F}^T\mathbf{F}$, provides us with information on the effect of small changes in various rate constants of the mechanism on the objective function. In this way it is possible to identify those reactions important to the observed behavior at a certain time and additionally, one can reveal the major reaction interactions (e.g., equilibria, quasi-steady-state) of the model studied. These results, combined with other methods that are to be discussed later, also guide the elimination of redundant reactions and species thus the simplification of the mechanism.

The GTF mechanism was analyzed and simplified using the numerical reproduction of three batch experiments from our previous paper.[4] These were preferred over some arbitrary conditions since they are numerical simulations of carefully conducted real experiments in oxygen-free solution. The experiments studied were performed using rather different chemical conditions, so our conclusions should be valid for a wide range of other experiments done with the classic BZ system. All the analysis to be discussed below was carried out simultaneously with these three test simulations, and the results were evaluated by putting the emphasis on features in common.

Figure 1 shows the log [Br⁻] curve of the three test cases. The initial concentrations of these simulations (identical to experiments) are as follows:

Case 1:[18] $[BrO_3^-] = 0.1$ M, [MA] = 0.6 M, [Ce(III)] = 0.001 M, $[H^+] = 1.29$ M, [OA] = 1×10^{-6} M (Figure 1A)

Case 2:[8] $[BrO_3^-] = 0.1$ M, [MA] = 0.4 M, [Ce(III)] = 0.02 M, $[H^+] = 1.29$ M (Figure 1B)

Case 3:[19] $[BrO_3^-] = 0.1$ M, [MA] = 0.28 M, [Ce(III)] = 0.0005 M, $[H^+] = 1.29$ M, [HOBr] = 0.06 M (Figure 1C)

The analysis of the behavior of the model in these test cases and the first few steps of the simplification were performed following the scheme suggested by Turányi[16] for large reaction mechanisms. Skeleton models were constructed by first identifying species redundant for the reproduction of oscillations. When these species are removed from the mechanism a simple model results that can be further reduced by more traditional considerations of the reaction kinetics, i.e., by quasi-steady-state, fast-equilibrium and rate-determining-step assumptions.

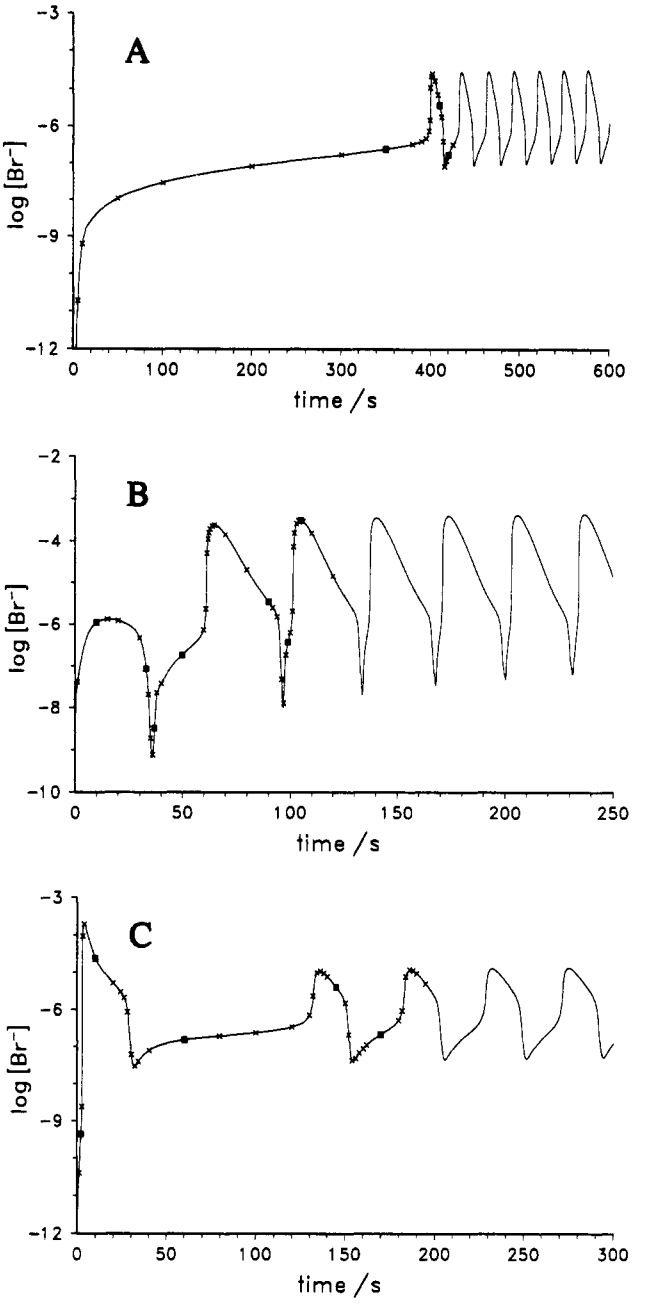

Figure 1. log[Br⁻] time series of the three test cases used in this work. Initial concentrations are specified in the text. Crosses indicate observation times for principal component analysis, solid squares indicate observation times representative for a certain kinetic regime. The observation times (in seconds) are as follows (underlined times indicate representative observation times). A. Case 1: 0.5 (not shown), 1 (not shown), 2 (not shown), 5, 10, 50, 100, 200, 300, 350, 380, 390, 395, 398, 399, 400, 401, 402, 405, 408, 410, 412, 414, 416, 418, 420, 425. B. Case 2: 1, 10, 15, 20, 30, 33, 34, 35, 36, 37, 38, 40, 50, 60, 61, 61.5, 62, 62.5, 63, 64, 65, 70, 80, 90, 92, 94, 96, 97, 98, 99, 100, 101, 101.5, 102, 103, 104, 105, 106, 110, 120. C. Case 3: 1, 2, 2.5, 3, 4, 10, 20, 24, 26, 28, 30, 32, 34, 40, 60, 80, 100, 120, 130, 132, 134, 136, 138, 140, 145, 150, 152, 154, 156, 158, 160, 162, 170, 180, 182, 184, 186, 188, 190, 195.

Major Reaction Structures of the GTF Model. To identify major reaction structures of the model the PCA has to be performed with all species of variable concentration in the objective function.[15] This was done with the full GTF mechanism in all

the three cases at instants marked with crosses in Figure 1. Based on the results of this analysis the observation times were grouped so that the major reaction structures are the same within each group. Representative observation times for these groups were chosen and are marked by solid squares in Figure 1. Over 40 reaction clusters were found in the three test simulations. In the following the most important of these are discussed. They are either fast equilibria or reaction chains connected via species for which the quasi-steady-state may be assumed.

Reactions that are always or almost always grouped together. The first of these structures is the MA ⇄ ENOL equilibrium (reactions 15 and 16). This fast equilibrium is established in all three test simulations.

Another fast equilibrium that almost always holds is that of reactions 59 and 60, a radical transfer between malonyl radical and tartronic acid. The only time this equilibrium is shifted towards the production of malonyl radical is during some very oxidative stages when other reactions (e.g., reaction 27) produce significant amounts of TTA•.

A quasi-steady-state assumption for •COOH radical connects reaction 29 to reactions 53 and 71. This connection holds in all three test cases and it is an important chain by which bromide is liberated from bromomalonic acid. This has interesting consequences for the debate about the stoichiometric factor of the Oregonator model.[20,21] Depending on the ratio [BrMA]/[Ce(IV)] the production of one bromide via this chain may need one to two Ce(IV). The source of •COOH in reaction 29 is mesoxalic acid (MOA) that is produced primarily in reactions 22 and 24. Reaction 22 is the key reaction of the "radical control", since this way a BrO_2• radical is reduced to HOBr. Reaction 24 is the decomposition of bromotartronic acid. One molecule of BrO_2MA is produced by using only one Ce(IV) ion and one molecule of BrTTA is produced using one to two Ce(IV). Consequently, if the [BrMA]/[Ce(IV)] ratio is high enough it is possible to produce one bromide ion per two to three Ce(IV) ions as is assumed in the Oregonator model. Also note, that reaction 71 produces a malonyl radical (MA•) that may go on to react with BrO_2• in reaction 46 or with BrMA in reaction 61 to produce another MOA thus potentially reducing the Ce(IV)/Br^- ratio below 2!

There is yet another pathway that is valid through the oscillatory phases of these simulations and that produces more than one Br^- per Ce(IV). A quasi-steady-state assumption for bromine atom connects reaction 56 to reactions 75 and 77. These reactions can be grouped together into the general form:

$$Q + R^\bullet + Br_2 \rightarrow Br^- + Q^\bullet + RBr$$

where R• and Q• are organic radicals. This means that once a malonyl radical is produced in the system there is a radical-catalyzed bromide production from bromine via bromine atoms that involves BrMA or MA as the source of the product radical.

Even at early stages of the study of the inorganic reaction subset of the BZ reaction it was assumed that BrO_2• is always at equilibrium with Br_2O_4, thus reactions 9–12 were combined into a single equilibrium:

$$BrO_3^- + HBrO_2 + H^+ \rightleftarrows 2\ BrO_2^\bullet + H_2O$$

Our studies show, that this assumption is not valid during the reduced stage of tests 1 and 2 where a QSSA holds for Br_2O_4 between reactions 9 and 11. This only means that the reverse of the above reaction is negligible in these cases and it does not affect the rate equation that should be used for this process.

Reaction clusters appearing at some particular phases of the simulations. In case 2 during the oscillatory part of the simulations a QSSA holds for BrMA• as reaction 77 produces and reactions 38 and 39 consume it. Since BrTTA (the product of both consuming reactions) releases a bromide ion, in this cluster of reactions two bromides are produced by consuming less then two Ce(IV) ions if we assume that Br• is produced in reactions 26 followed by 56.

During the oxidative stage of the oscillations in tests 2 and 3 a quasi-steady-state assumption holds for Br_2 involving reactions 1 and 17. This means that most of the bromine formed in reaction 1 goes on to quickly brominate malonic acid. Furthermore, during the oscillations in test 1 a quasi-steady-state can be assumed for HOBr between reactions 3 and 1. Although, the two QSSA's do not hold simultaneously, the fact that they both can be identified as important reaction structures of the BZ mechanism supports the assumptions of Györgyi and Field[13,14] who originated BrMA from reaction 3 by eliminating the variables Br_2 and HOBr when they derived simple chaotic models of the BZ reaction.

The last important reaction cluster (26, 61, 46, 39) is brought together by a QSSA for MA• followed by a QSSA for BrMA• and exists during the oxidative stage of tests 1 and 3. In this reaction sequence Ce(IV) oxidizes MA in reaction 26. The resulting MA• reacts either in reaction 46 or in reaction 61. The BrMA• produced in reaction 61 goes on to react with BrO_2• to yield BrTTA and eventually a bromide ion. This group is a particularly nice combination of the two proposed negative feedback mechanisms of this system. A radical-control step (46) occurs simultaneously with the production of the originally-thought control intermediate bromide from BrTTA. (Note that reaction 61 is not an inhibition of the $HBrO_2$ autocatalysis.)

Simplification of the GTF Model. *Derivation of the 42-Reaction Mechanism.* The first step in a reaction rate sensitivity assisted simplification procedure[16] is the separation of the components of the mechanism into three disjunct groups. The first is called "important species" and we define them as the ones that are either initial reagents or those that can be more or less quantitatively measured in the system. These are Br^-, Ce(IV), BrO_3^-, MA, Br_2, CO_2, $HBrO_2$, BrMA, MA•. The second group is called the "necessary species" and these are the ones needed in the mechanism to quantitatively reproduce the behavior of the full model. The remaining components are called "redundant species". A PCA performed on the full model, but only with the important and necessary species in the objective function identifies the redundant reactions that can be eliminated without major change in the observed behavior.

The consuming, then both the consuming and producing reactions of the non-important components of the GTF mechanism were removed[16] and the agreement with the full model was checked in all three test cases. This procedure yields three redundant species: TTA, TTA• and BrO_2TTA. Note that Br_2MA is only a product component that is not listed among the important species, thus it can be eliminated from the mechanism without any consequences. The PCA was then performed at the representative instants shown by solid squares in Figure 1 with the non-redundant components in the objective function. Those reactions were considered to be important in the simulation of the observed behavior which appear as large elements (>0.2 in absolute value) in eigenvectors with eigenvalues larger than 0.01, and are not consuming reactions of any redundant species. The results are detailed in Figure 2. Columns belong to the representative observation times, while rows represent the reactions of the model. Columns S and SS are used to summarize the results as follows. Shading in a row indicates that the reaction represented by the row is important at the instant represented by the column in which the shading occurs. A filled circle in column S marks those reactions that are important at any instant in a certain test simulation. Boxed reaction number and a cross in column SS marks the reactions important at any time in any of the tests. The reduced models contain 37, 36 and 31 reactions for cases 1, 2, and 3, respectively. The combined model (boxed numbers and cross in column SS) has 42 reactions and 22 components. This model reproduces the behavior of the original 80-reaction model very well as is shown in Figure 3.

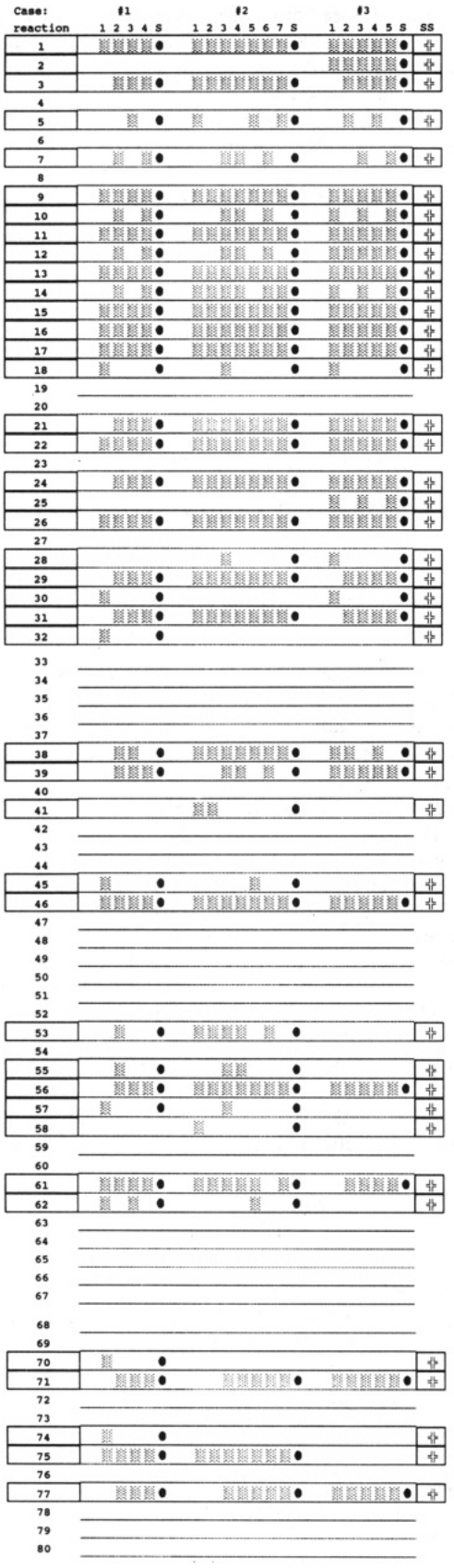

Figure 2. Reaction importances during various phases of the three test simulations as a result of the principal component analysis with important and necessary species in the objective function. The numbers in the header indicate the index of observation time representative for a certain kinetic regime (solid squares in Figure 1), column S indicates the summary of a particular test case, while column SS is the summary for all test cases. A cross in the SS column and a box around the reaction number indicate reactions that are important in any of the test simulations, thus are part of the 42-reaction mechanism.

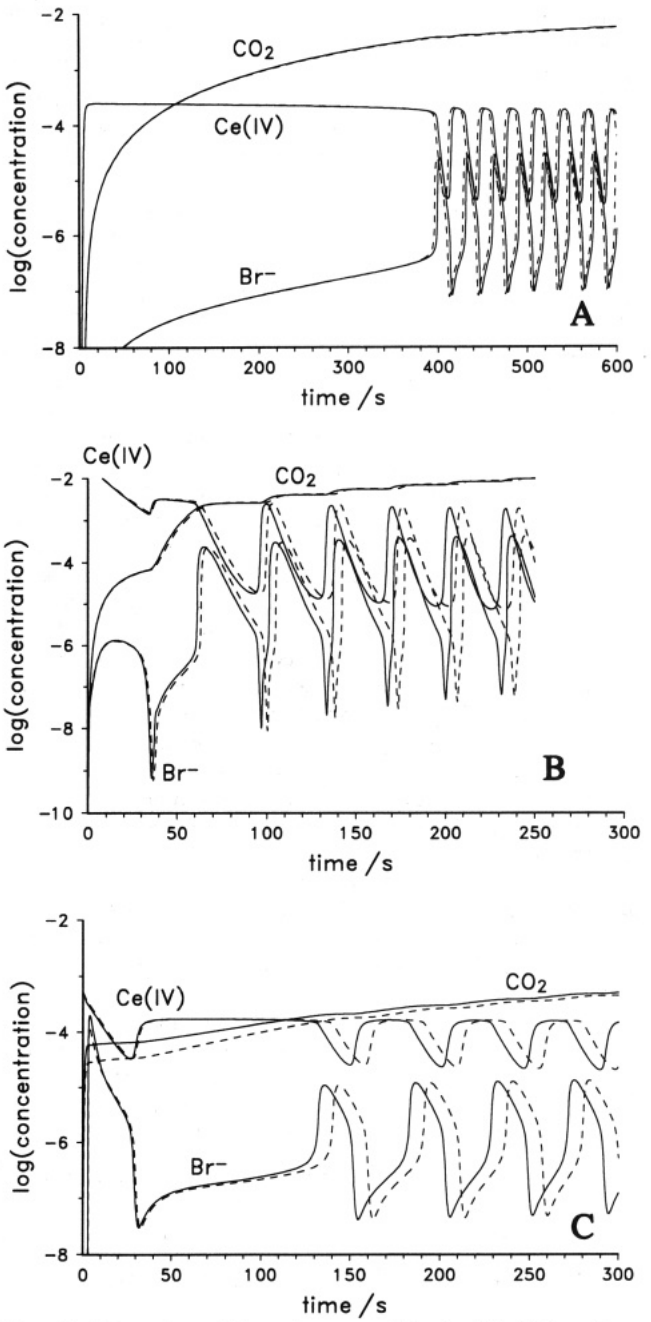

Figure 3. Comparison of the performance of the simplified 42-reaction, 22-species mechanism (dashed line) with the original GTF mechanism (solid line) in the three test simulations. A. Case 1. B. Case 2. C. Case 3.

Skeleton Models. The goal of this stage of the simplification procedure was the identification of the minimal set of reactions and components that still produce sustained, limit-cycle oscillations in the concentration of Br^- and Ce(IV) under the conditions of the transient oscillations observed in the three test simulations. The above components were singled out as those measured in the vast majority of BZ experiments. We also point out that no built in assumption about the form of the resulting simple models is contained in the simplification procedure.

The time periods that were chosen for qualitative reproduction are 425–600 s in case 1, 110–250 s in case 2, and 145–300 s in case 3. The initial conditions for the simulations to be described here were those calculated from the full model at the starting times listed above. Since the goal was to obtain models that produce limit-cycle oscillations we used the pool-component approximation for a number of species with large concentration, specifically for MA, BrO_3^-, H^+ and BrMA with their concen-

tration kept at the initial value described above. Carbon dioxide is only a product component in the 42-reaction model, thus it can be removed at this stage without any consequences.

The first stage of the search for simple models was a systematic elimination of first the consuming then both the consuming and producing reactions of all components expect for the pool components, Br^- and Ce(IV). A reduced model that still oscillates in all cases is obtained by eliminating the consuming reactions of HOBr, MOA and OA and both the consuming and producing reactions of $Br^•$, BrO_2MA, and $^•COOH$. Repeating the above procedure with this model reveals that the consuming reactions of Br_2 can also be removed (note that BrMA is already a pool component) and another iteration of this procedure fails. Note that the elimination of reaction 17 (bromination of ENOL to yield BrMA) above allows the removal of reactions 15, 16 (enolization equilibrium) and the ENOL form of MA from the mechanism. Furthermore, Figure 2 shows that reactions 70 and 45 are not important during the oscillations in any of the cases, and reactions 25 and 62 are important only at one representative oscillatory observation time. A control simulation proved that all the four reactions above can be eliminated without losing the oscillatory behavior of the model. The resulting mechanism contains the following reactions: 3, 5, 7, 9-14, 24, 26, 38, 39, and 61; and the species: Br^-, $HBrO_2$, Ce(IV), Ce(III), $BrO_2^•$, Br_2O_4, BrTTA, $MA^•$, and $BrMA^•$. This model is noted as model A.

Before proceeding, we remark that two important conclusions can be drawn at this stage. One is, that the radical control in reactions 46, 21, and 22 is not necessary to reproduce the oscillations in this model. Second, the oxidation of BrMA by Ce(IV) is not the major initiation of Br^- production as indicated by the possible elimination of reaction 25.

In model A there are two reactions that converts $BrMA^•$ to BrTTA: reactions 38 and 39. The elimination of reaction 39 does not cause any change in case 2 and causes only a minor change in the period in cases 1 and 3. On the other hand, reaction 38 can not be eliminated without a several fold increase in the period (cases 1 and 2) or the cessation of oscillations (case 3). Thus the next model, model B, is model A without reaction 39.

The reaction chain that generates bromide in model B consists of the following steps (curly brackets indicate pool components, slashes indicate components eliminated previously):

$$\text{Ce(IV)} + \{\text{MA}\} \rightarrow \text{Ce(III)} + \text{MA}^• + \{\text{H}^+\} \quad (26)$$

$$\text{MA}^• + \{\text{BrMA}\} \rightarrow \{\text{MA}\} + \text{BrMA}^• \quad (61)$$

$$\text{BrMA}^• + \text{Ce(IV)} + \{\text{H}_2\text{O}\} \rightarrow \text{BrTTA} + \text{Ce(III)} + \text{H}^+ \quad (38)$$

$$\text{BrTTA} \rightarrow \text{Br}^- + /\text{MOA}/ + \{\text{H}^+\} \quad (24)$$

Further simplification is possible if we assume that the rate determining step of this chain is reaction 26. In the presence of sufficient amounts of BrMA (as is the case in most BZ systems under oscillatory conditions) this is a reasonable assumption. Thus we replace reactions 26, 61, 38, 24 with a single step:

$$\text{Ce(IV)} + \{\text{MA}\} \rightarrow 2\text{Ce(III)} + \text{Br}^- + \{3\text{H}^+\} + \{\text{MA}\} + /\text{MOA}/ - \text{Ce(IV)} - \{\text{BrMA}\} \quad (81)$$

$$\text{with} \quad k_{81} = k_{26}$$

In reaction 81 and elsewhere in this work negative stoichiometric numbers describe the exact material balance while maintaining the mass-action-kinetics structure of the model. Their use is quite common, e.g., in smog models. The use of reaction 81 also eliminates three species: $MA^•$, $BrMA^•$ and BrTTA. Thus we obtain the next simple model, model C, with reactions: 3, 5, 7, 9–14, 81; components: Br^-, $HBrO_2$, Ce(IV), Ce(III), $BrO_2^•$, Br_2O_4.

It has already been discussed in some details in the analysis of the GTF model that reactions 11 and 12 form a fast equilibrium most of the time, and when this is not the case then reactions 10 and 12 are much slower than 9 and 11. The rate determining step is reaction 9 in this latter case. This allows us to replace reactions 9–12 with the equilibrium reaction

$$\text{BrO}_3^- + \text{HBrO}_2 + \text{H}^+ \rightleftarrows 2\,\text{BrO}_2^• + \text{H}_2\text{O} \quad (82,83)$$

where $k_{82} = k_9 = 33.0\ M^{-2}\ s^{-1}$, and $k_{83} = k_{10}(k_{11}/k_{12}) = 4.2 \times 10^7\ M^{-1}\ s^{-1}$. This results in model D that contains the following reactions:

$$\text{HBrO}_2 + \text{Br}^- + \{\text{H}^+\} \rightarrow /2\text{HOBr}/ \quad (3)$$

$$\text{Br}^- + \{\text{BrO}_3^-\} + \{2\text{H}^+\} \rightarrow \text{HBrO}_2 + /\text{HOBr}/ \quad (5)$$

$$2\text{HBrO}_2 \rightarrow \{\text{BrO}_3^-\} + /\text{HOBr}/ + \{\text{H}^+\} \quad (7)$$

$$\text{HBrO}_2 + \{\text{BrO}_3^-\} + \{\text{H}^+\} \rightleftarrows 2\,\text{BrO}_2^• + \{\text{H}_2\text{O}\} \quad (82,83)$$

$$\text{Ce(III)} + \text{BrO}_2^• + \{\text{H}^+\} \rightleftarrows \text{Ce(IV)} + \text{HBrO}_2 \quad (13,14)$$

$$\text{Ce(IV)} + \{\text{MA}\} \rightarrow 2\text{Ce(III)} + \text{Br}^- + \{3\text{H}^+\} + \{\text{MA}\} + /\text{MOA}/ - \text{Ce(IV)} - \{\text{BrMA}\} \quad (81)$$

A comparison of the performance of models B, C, and D with that of the GTF mechanism on the three test cases indicates that both the period and the shape of the oscillations are largely preserved during the simplification procedure.

We now derive three skeleton models from model D. To do this, we eliminate two more components of variable concentration, Ce(III) ions and $BrO_2^•$. In the classic Oregonator reactions 83 and 14 were ignored, and QSS was assumed for $BrO_2^•$ as reaction 82 produces and reaction 13 consumes it. This assumes that the rate determining step of this autocatalytic process is reaction 82 and the concentration of Ce(III) ions does not appear in the rate equations. Experimental study[22] of the inorganic subset of the BZ reaction indicated that the autocatalytic reaction between BrO_3^- and $HBrO_2$ is reversible to a great extent under conditions characteristic to the BZ system. This means that reactions 83 and 14 can not be ignored. Using the classic simplifying assumptions of reaction kinetics there are two alternatives[13] for elimination of $BrO_2^•$ radical. In the first approach it can be assumed that reactions 82 and 83 are in equilibrium at most of the time, thus

$$[\text{BrO}_2^•]_{\text{EQ}} = \left(\frac{k_{82}}{k_{83}}[\text{BrO}_3^-][\text{H}^+]\right)^{1/2}([\text{HBrO}_2])^{1/2}$$

The more accurate assumption is the QSSA. It takes into consideration all the processes that affect the concentration of $BrO_2^•$ and results in the formula

$$[\text{BrO}_2^•]_{\text{QSS}} = \frac{1}{2}\left\{\frac{k_{13}}{2k_{83}}[\text{H}^+][\text{Ce(III)}] + W\right\}$$

where

$$W = \left[\left(\frac{k_{13}}{2k_{83}}[\text{H}^+][\text{Ce(III)}]\right)^2 + \frac{4[\text{HBrO}_2]}{k_{83}}\left(k_{82}[\text{BrO}_3^-][\text{H}^+] + \frac{k_{14}}{2}[\text{Ce(IV)}]\right)\right]^{1/2}$$

The Ce(III) concentration in these two cases can be calculated from the mass balance: $[\text{Ce(III)}] = [\text{Ce}]_{\text{tot}} - [\text{Ce(IV)}]$, where $[\text{Ce}]_{\text{tot}}$ is the total catalyst concentration added to the system. The resulting two models are shown in Table II. They have the same stoichiometry, the only difference between them is the way $[\text{BrO}_2^•]_{\text{est}}$ is calculated, as described above. The model with the

TABLE II: Skeleton Models of the BZ Reaction (Model E and Model F)[a]

	reaction	rate expression
EF-1	$X + Y + \{H\} \rightarrow /2P/$	k_3hxy
EF-2	$Y + \{A\} + \{2H\} \rightarrow X + /P/$	k_5ah^2y
EF-3	$2X \rightarrow /P/ + \{A\} + \{H\}$	k_7x^2
EF-4	$0.5X + \{A\} + \{H\} \rightarrow X + Z$	$k_{13}(c - z)u_{est}h$
EF-5	$X + Z \rightarrow 0.5X + \{A\} + \{H\}$	$k_{14}xz$
EF-6	$Z + \{M\} \rightarrow Y - Z$	$k_{26}mz$

[a] In Model E equilibrium assumption, while Model F quasi-steady-state assumption is used to estimate $[BrO_2^{\bullet}]$ (see text for details). The indices of the rate constants refer to Table I. A notation similar to that of the Oregonator model was used for comparison: $X \equiv HBrO_2$, $Y \equiv Br^-$, $Z \equiv Ce(IV)$, $A \equiv BrO_3^-$, $H \equiv H^+$, $P \equiv HOBr$, $M \equiv MA$. Curly brackets indicate pool components, slashes inert products. In the rate expressions lower case letters denote the concentration of the given species, c is the total Ce ion concentration and u_{est} refer to the estimated concentration of $BrO_2^{\bullet}$.

TABLE III: Skeleton Model of the BZ Reaction (Model G)[a]

	reaction	rate expression
G-1	$X + Y + \{H\} \rightarrow /2P/$	k_3hxy
G-2	$Y + \{A\} + \{2H\} \rightarrow X + /P/$	k_5ah^2y
G-3	$2X \rightarrow /P/ + \{A\} + \{H\}$	k_7x^2
G-4	$X + \{A\} + \{H\} \rightarrow 2X + 2Z$	k_9ahx
G-5	$X + Z \rightarrow 0.5X + \{A\} + \{H\}$	$k_{14}xz$
G-6	$Z + \{M\} \rightarrow Y - Z$	$k_{26}mz$

[a] The indices of the rate constants refer to Table I. A notation similar to that of the Oregonator model was used for comparison: $X \equiv HBrO_2$, $Y \equiv Br^-$, $Z \equiv Ce(IV)$, $A \equiv BrO_3^-$, $H \equiv H^+$, $P \equiv HOBr$, $M \equiv MA$. Curly brackets indicate pool components, slashes inert products. In the rate expressions lower case letters denote the concentration of the given species.

equilibrium assumption is model E, the one with the QSSA is model F. Model E fails to oscillate in tests 2 and 3 with the rate constants of the GTF mechanism and with the initial conditions extracted from the three test simulations. Thus we will focus on model F in the following sections.

Although the derivations of models E and F are well based on the accepted simplifying methods of reaction kinetics the models lack the conceptual and structural simplicity of the classic Oregonator model. With somewhat more arbitrary assumptions, however, it is possible to derive a model that is as simple as the Oregonator and still approximates the behavior of the GTF mechanism reasonably well. Table III shows model G that is a purely mass-action-kinetics skeleton of the GTF mechanism. Its derivation assumes that the reaction sequence (82, 83) followed by (13, 14) is stoichiometrically reversible, but the rate determining step is reaction 82 in the forward direction and reaction 14 in the reverse direction. This is a similar assumption to that of the Oregonator in that it also makes the concentration of Ce(III) ion eliminable from the mechanism without invoking the mass conservation, and that it assumes that the rate determining step of the $HBrO_2$ autocatalysis is reaction 9. The difference is the reverse stoichiometry represented by the sequence (14, 83). Although Model G is not an "official offspring" of the GTF mechanism it performs well in reproducing the oscillations and it is an improvement over the Oregonator model.

A comparison of the oscillations generated by the skeletons, Models F and G, and by the Oregonator with those seen in the GTF mechanism is shown in Figures 4 and 5. The Oregonator model used in these simulations is shown in Table IV for reference. The Field–Försterling[22] rate constant values were assigned to the first four reactions of the Oregonator. These are identical with those used in the GTF mechanism. Figure 4 shows time series, so that the period of the various models can be compared, while Figure 5 displays the log[Br⁻]–log[Ce(IV)] phase-plane so that the waveform and relative phases can be seen. In Figure 5 the limit-cycle behavior of the skeletons is compared to the transient oscillations of the GTF mechanism as was originally done with the Oregonator model.

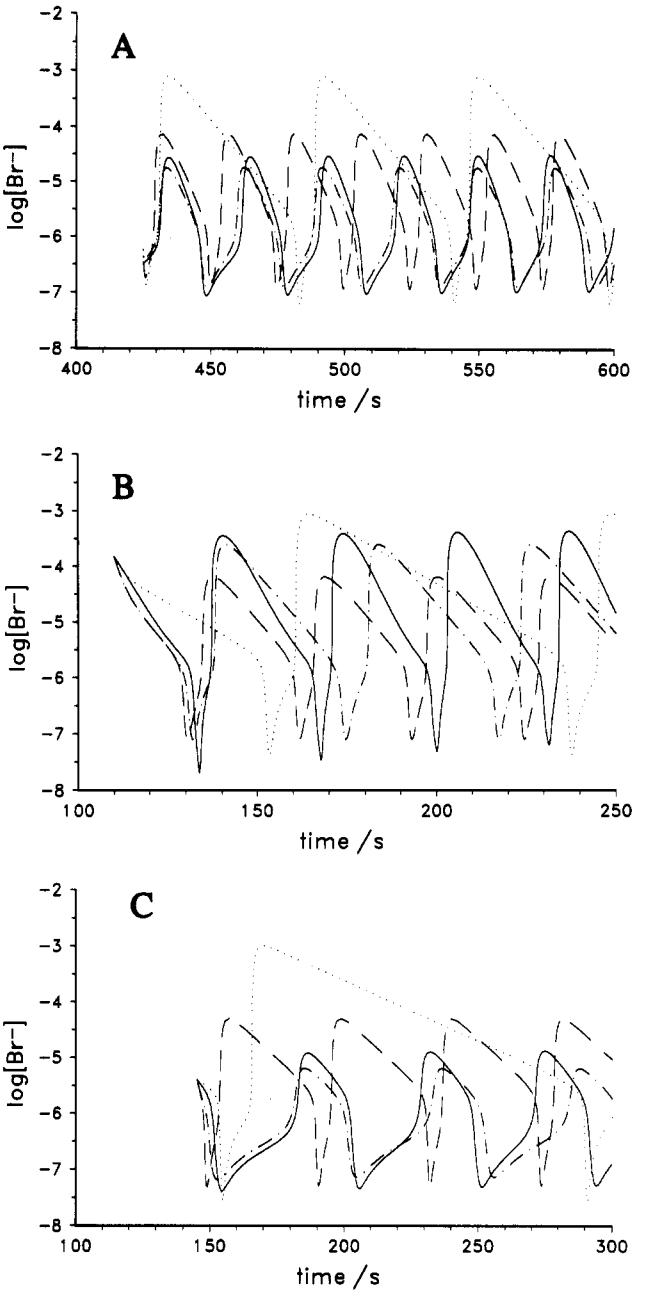

Figure 4. Comparison of the log[Br⁻] time series generated by model F (dot-dash line) and model G (dashed line) obtained in this work and by the Oregonator (dotted line) with the transient oscillations found with the GTF mechanism (solid line). A. Case 1. Pool component concentrations: $[BrO_3^-] = 0.0866$ M, $[H^+] = 1.3$ M, $[MA] = 0.5739$ M, $[Ce]_{tot} = 0.001$ M. B. Case 2. Pool component concentrations: $[BrO_3^-] = 0.0895$ M, $[H^+] = 1.3$ M, $[MA] = 0.3696$ M, $[Ce]_{tot} = 0.02$ M. C. Case 3. Pool component concentrations: $[BrO_3^-] = 0.0986$ M, $[H^+] = 1.3$ M, $[MA] = 0.2174$ M, $[Ce]_{tot} = 5 \times 10^{-4}$ M.

Discussion

The GTF model is so far the most complete chemical mechanism of the classic BZ reaction. Although many of the reactions suggested in it had already been studied, a great number of them were assumed by analogy and by chemical intuition. The 42-reaction subset presented here contains processes necessary for the quantitative reproduction of the three test simulations. Although other processes may become important if a system with very different initial composition is studied, this subset seems to contain much of the major reactions of the GTF mechanism. This allows us to pinpoint at those reactions and intermediates that seem to be important but lack experimental support. We hope this may guide the design of future experiments on this system.

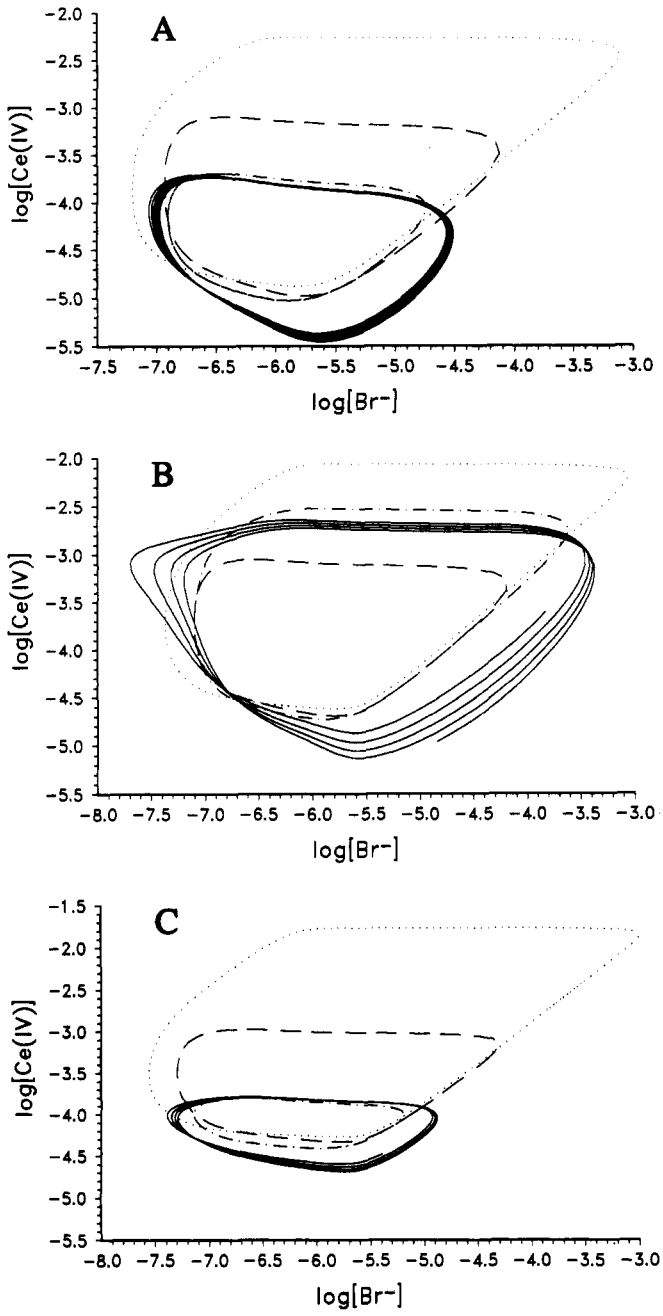

Figure 5. Comparison of the limit cycle in the log[Br⁻]–log[Ce(IV)] phase plane of model F (dot–dash line) and model G (dashed line) obtained in this work and that of the Oregonator model (dotted line) with the transient oscillations found with the GTF mechanism (solid line). Pool component concentrations are as in Figure 4. A. Case 1. B. Case 2. C. Case 3.

TABLE IV: Oregonator Model of the BZ Reaction with the Field–Försterling[22] Rate Constants[a]

	reaction	rate expression
O-1	$X + Y + \{H\} \rightarrow /2P/$	k_3hxy
O-2	$Y + \{A\} + \{2H\} \rightarrow X + /P/$	k_5ah^2y
O-3	$2X \rightarrow /P/ + \{A\} + \{H\}$	k_7x^2
O-4	$X + \{A\} + \{H\} \rightarrow 2X + Z$	k_9ahx
O-5	$Z + M \rightarrow Y$	$k_{26}mz$

[a] The indices of the parameters refer to Table I. The notation used is: X ≡ $HBrO_2$, Y ≡ Br^-, Z ≡ 2Ce(IV), A ≡ BrO_3^-, H ≡ H^+, P ≡ HOBr, M ≡ MA. Curly brackets indicate pool components, slashes inert products. In the rate expressions lower case letters denote the concentration of the given species.

(1) The bromination of malonic acid by HOBr (reaction 18) is not yet proven to occur as a direct reaction between these two species. As in the case of bromination with Br_2, the reaction is expected[3] to occur between the enol form of MA and HOBr. Experiments[3] in the presence of Ag^+ indicate that bromination takes place even at very low [Br^-].

(2) The radical species •COOH is still important in the 42-reaction scheme. Neither its existence nor the reactions of oxalic acid and mesoxalic acid that produce it are experimentally verified yet. Its importance as a reducing agent has to be proven too.

(3) Although it seems very probable that such a species exist, BrTTA produced by the two electron oxidation of BrMA, is also an assumed species. It has a great importance in the bromide production pathway of the GTF mechanism.

(4) The analysis and the simplification presented here clearly proved that there is a place for the radical inhibition steps (reaction 46 followed by reactions 21 and 22) in a complete BZ mechanism. The exact form of this inhibition is not yet proven though, in that the existence of BrO_2MA and its decomposition products need to be found experimentally. The two way decomposition used in the GTF model and the ratio k_{21}/k_{22} is the result of numerical fitting of experiments done with the complete BZ system, thus it is possible, that the above complex decomposes in some other way. If this results in the reduction of $BrO_2^•$ to Br^- then the inhibition by MA• is accompanied with the production of an additional inhibitory species, Br^-. It has to be mentioned here that the radical inhibition seems to lose its importance when the emphasis is on the reproduction of the oscillations in the usual BZ medium, ≈1 M H_2SO_4. It may contribute to the details of the waveform of the oscillations but it is clearly redundant in bringing them about in the GTF mechanism.

One reaction that is very important all along the simplification process is the radical transfer between malonyl radical and BrMA (reaction 61). It had already been suggested to be important in these systems by Jwo and Noyes[23] and was recently studied by Försterling and Stuk.[10] Unfortunately, in the first experimental work[23] O_2 was not excluded from the solutions thus their results can not be directly compared to those of the Försterling–Stuk experiments where the reaction mixtures were deoxygenated. In their flow-cell ESR experiments Försterling and Stuk observed that the addition of BrMA does not decrease the steady state MA• concentration. When the flow is stopped, however, [MA•] decreases faster if BrMA is present. From the flow experiments they concluded that the radical transfer reactions are unimportant, but they also acknowledge, that then there is no good explanation for the stopped-flow phenomena. They did not mention in their work the experiments of Jwo and Noyes[23] indicating that processes like reaction 61 should occur (they studied the oxidation of various mixtures of organic species important in the BZ reaction by Ce(IV)).

Since these reactions seem to be essential in the GTF mechanism, and similar radical transfer reactions are fairly common,[24] in the Appendix we present an interpretation of the experiments of Försterling and Stuk[10] that contains the radical transfer steps. We do this by adding the hydrolysis reaction of BrMA•:

$$BrMA^• + H_2O \rightarrow TTA + Br^- \qquad (84)$$

to the GTF mechanism and with this semiquantitatively reproduce both sets of ESR experiments.[10] We suggest that the jury is still out in this question and that if reaction 61 is to be disregarded then alternative explanation should also be provided for the experiments of Jwo and Noyes.[23]

Reaction 38, the reaction between Ce(IV) and BrMA•, has an important role in the GTF mechanism and is directly or indirectly included in all the reduced models. The above mentioned experiments of Försterling and Stuk and also those of Jwo and Noyes indicate that this reaction does not contribute to the reduction of Ce(IV) by BrMA. One possible substitute for this process is reaction 84. If reaction 38 is replaced by reaction 84 the bromide producing pathway becomes very similar to the one

found in this study except for a change in the stoichiometry. In this case one Ce(IV) is enough to generate a bromide ion. This change is expected to have major consequences on the observed behavior and will have to be a subject of further studies.

There is another work of Försterling and Stuk that needs to be considered here. In a recent report[11] they study reaction 41, the disproportionation of MA•. In the usual BZ medium (1 M H_2SO_4) they found $k_{41} = 4.2 \times 10^8$ M^{-1} s^{-1} that is about 13% of the value[25] used in the GTF model. Since much of the rate constants of radical-radical reactions in the GTF mechanism were estimated by analogies with the previous value of k_{41} in a future refinement these values should also be lowered.

Another topic investigated in the above paper[11] is the effect of the formation of the sulfato complexes of Ce(IV) on the rate of oxidation of organic material by Ce(IV). They found that our suggestion,[4] in that some peculiarities of the BZ kinetics could be due to the fact that uncomplexed Ce(IV) may also react with organic material, is not supported by their experiments, Ce(IV) complexes are formed on a much faster timescale than that of the oxidation processes. Based on the experimental work of Jwo and Noyes[23] we suggest another interpretation of some of the unexplained phenomena. The above authors observe the following: (1) The oxidation of those organic molecules that does not have two carboxyl or a carboxyl and an adjacent carbonyl groups is negligible when compared to those bearing these structural features. (2) The oxidation of organic radicals in systems containing significant amounts of the original organic material (from which the radicals originated) by Ce(IV) is most probably negligible when compared to their disproportionation (this suggestion was independently confirmed in the case of BrMA• by Försterling and Stuk[10]). (3) The oxidation of BrMA by Ce(IV) is slowed down significantly as increasing amounts of H_2SO_4 or $KHSO_4$ was added to the $HClO_4$ medium.

Jwo and Noyes suggest that the oxidation of organic matter occurs via the formation of bidentate complexes with Ce(IV) as an explanation for the first two observations. This is, in fact, in agreement with the third fact too, where a competition between sulfate ion and the organic matter for complexing Ce(IV) may reduce the apparent rate of oxidation. Taking this idea one step further may be able to explain the peculiar facts discussed in our previous work[4] that seem to indicate that "freshly oxidized" Ce(IV) in the BZ medium reacts faster with organic material than Ce(IV) that is in equilibrium with ≈1 M H_2SO_4. In BZ systems it is only about 20–50 percentage of the total Ce concentration that is oxidized to Ce(IV) during one cycle of the oscillation. The rest remains as Ce(III) and may form the above mentioned chelate complexes with the organic materials present in large amounts. If this complex is not broken when Ce(III) is oxidized to Ce(IV) in reaction 13 then the oxidation of the already complexed organic material will be much faster in a reacting BZ medium than can be measured in an experiment where the organic is added to a Ce(IV) solution prepared in 1 M H_2SO_4.

Figures 4 and 5 indicate that two of the skeleton models derived here works better in reproducing the sustained oscillations of the test experiments than the original Oregonator model.[12] In Table V we provide a quantitative comparison in all test cases in terms of the value of [Br⁻] extrema, the time elapsed between them within one cycle and the length of a full oscillation. These data adequately describe the shape of the [Br⁻] time series. It should also be mentioned here that while the Oregonator is only a "pseudo-mass-action-kinetics" model ($Z \equiv 2Ce(IV)$, $z = 2[Ce(IV)]$), the differential equations describing model G of this work can be derived solely on the basis of mass-action-kinetics.

It is apparent from Figures 4 and 5 and Table V that model F generally performs better than model G, though this latter one does very well for its simplicity. It is surprising that model E (not shown in Table V) fails to oscillate in two cases. The equilibrium assumption used in its derivation has been successful already when chaotic BZ mechanisms were simplified.[13,14] In those cases, however, it was not required that the phenomena exhibited by the original model be reproduced at exactly the same parameter values, and indeed, the chaos occurs at higher flow rates in the simple model with the equilibrium assumption then in the original mechanism. We also made small changes in the parameterization of model E to see if oscillations can be reproduced at slightly different values of its rate constants. It was found that less than a factor of two increase in [MA] (i.e., [MA] = 0.6428 M and [MA] = 0.2836 M in cases 2 and 3, respectively) allows limit cycle oscillations to occur. Thus while model E does not stand the strict test of reproducing sustained oscillations under conditions identical with the test simulations, it should not be discarded as a possible tool for studying the dynamics of this system.

TABLE V: Comparison of the Performance of Model F, Model G, and the Oregonator Model with the Transient Oscillations Simulated with the GTF Model in Table I[a]

	$[Br^-]_{max}$ (M)	$[Br^-]_{min}$ (M)	t(max→min) (s)	t(min→max) (s)	period (s)
		Case 1			
GTF model	2.72×10^{-5}	8.63×10^{-8}	14.04	16.20	30.24
model F	1.83×10^{-5}	1.25×10^{-7}	14.99	13.94	28.93
model G	7.64×10^{-5}	1.17×10^{-7}	17.92	6.15	24.07
Oregonator	7.76×10^{-4}	6.22×10^{-8}	48.80	8.88	57.68
		Case 2			
GTF model	3.50×10^{-4}	2.02×10^{-8}	27.39	6.66	34.05
model F	2.43×10^{-4}	7.90×10^{-8}	33.52	9.15	42.67
model G	6.48×10^{-5}	7.93×10^{-8}	24.25	7.07	31.32
Oregonator	8.60×10^{-4}	4.27×10^{-8}	72.52	11.58	84.10
		Case 3			
GTF model	1.20×10^{-5}	4.10×10^{-8}	19.45	31.75	51.20
model F	6.47×10^{-6}	7.23×10^{-8}	19.73	32.03	51.76
model G	5.02×10^{-5}	5.29×10^{-8}	33.28	8.32	41.60
Oregonator	1.02×10^{-3}	2.78×10^{-8}	121.14	15.00	136.14

[a] The shape of the [Br⁻] oscillations is described with the maximum and minimum of [Br⁻], the time elapsed between them and with the period of the oscillations.

We would also like to point out that the skeleton models presented here do not contain any adjustable parameters, all the rate constants belong to well defined, simple reactions, and the values used here were all experimentally measured. The models contain explicitly the concentration of bromate ion, malonic acid and hydrogen ion. Models E and F also contain the total catalyst concentration. It is these parameters that give the models sufficient flexibility to reproduce a wide range of BZ experiments.

Concluding Remarks

The 80-reaction, 26-species GTF mechanism was thoroughly analyzed and reduced in this work to obtain a 42-reaction, 22-species mechanistic model and three different 3-variable skeleton models. The analysis of the reaction interactions revealed a number of reaction clusters that exist during most of the observed behavior. Among these are several reaction sequences that produce more than $^1/_2Br^-$ per Ce(IV). Interestingly, the simplification procedure resulted exactly in the ratio of $^1/_2Br^-$ per Ce(IV) as the dominant stoichiometry of bromide reproduction in the GTF mechanism that is also the optimal stoichiometry of the Oregonator model.

Nevertheless, it is also apparent from our analysis that the radical control by MA•, suggested as an additional negative feedback mechanism beside the bromide control manifested in the Oregonator, is also important for the complete reproduction of these experiments even if it is not necessary for the simulation of sustained oscillations.

The 42-reaction, 22-species model derived here performs as well as the original mechanism in the selected test simulations. It is suggested that the reactions of this model should be primarily investigated by experimentalists and additions should be tested

using this smaller set of reactions. Such a necessary addition to the GTF mechanism is reaction 84, the hydrolysis of bromomalonyl radical. This reaction is needed for the reproduction of several experiments performed with various subsystems of the BZ reaction. It is expected that the addition of this step will disturb the model, in that, it has to be refitted to several BZ experiments. This exceeds the scope of the present paper and is considered as a future project.

Several skeleton models of the BZ reaction have been introduced recently, some of them in this work. One may wonder which of them should be considered as the alternative of the Oregonator model. We suggest, that for the purposes for which the Oregonator was appropriate and where its simplicity was needed model G from this work should do very well. Model F offers better quantitative fit on the expense of lesser tractability. If complex oscillations or complete batch experiments (including induction period and the extinction of oscillations) should be modeled than the models derived here are not sufficient and recently introduced three- or four-variable schemes[13,14] could be used where [BrMA] serves as an additional variable. In those cases, again, one has to compromise between quantitative fit and simplicity.

Computations

All the calculations of the simplification procedure were carried out using KINAL,[26] a program package for the analysis of complex reaction mechanisms. The simulations aimed at the reproduction of the ESR experiments were done with the program SIMULATE, a simulation program for mass action kinetics written by one of us (L. Gy) that uses the integrator ROW4S.[27,28]

Acknowledgment. This work was supported by grants from the OTKA. We thank several of our distinguished colleagues who carefully read the manuscript. L.G. thanks Professor Endre Körös for his support.

Appendix

This appendix presents the detailed mechanism that was used to qualitatively and quantitatively interpret the ESR experiments of Försterling and Stuk.[10] All the reactions below, except for reaction 84, are contained in the GTF mechanism.

$$Ce(IV) + MA \rightarrow Ce(III) + MA^{\bullet} + H^{+} \quad (26)$$

$$Ce(IV) + BrMA \rightarrow Ce(III) + BrMA^{\bullet} + H^{+} \quad (25)$$

$$2MA^{\bullet} + H_2O \rightarrow MA + TTA \quad (41)$$

$$2BrMA^{\bullet} + H_2O \rightarrow BrMA + BrTTA \quad (35)$$

$$BrMA^{\bullet} + MA^{\bullet} + H_2O \rightarrow MA + BrTTA \quad (36)$$

$$Ce(IV) + BrMA^{\bullet} + H_2O \rightarrow Ce(III) + BrTTA + H^{+} \quad (38)$$

$$MA^{\bullet} + BrMA \rightleftarrows MA + BrMA^{\bullet} \quad (61,62)$$

$$BrTTA \rightarrow Br^{-} + MOA + H^{+} \quad (24)$$

$$Br^{\bullet} + MA \rightarrow Br^{-} + MA^{\bullet} \quad (75)$$

$$Ce(IV) + TTA \rightarrow Ce(III) + TTA^{\bullet} + H^{+} \quad (27)$$

$$MA^{\bullet} + TTA \rightarrow TTA^{\bullet} + MA \quad (59)$$

$$TTA^{\bullet} + MA^{\bullet} + H_2O \rightarrow 2TTA \quad (42)$$

$$2TTA^{\bullet} \rightarrow TTA + MOA \quad (47)$$

$$BrMA^{\bullet} + H_2O \rightarrow TTA + Br^{\bullet} \quad (84)$$

The first group of reactions (26–24) are those used by Försterling and Stuk to explain their ESR experiments and the second group (75–47) are additional reactions from the GTF mechanism. The fast hydrolysis reaction of $BrMA^{\bullet}$ (84) was originally suggested to occur by Jwo and Noyes.[23] Although these authors suggested different products ($TTA^{\bullet}$ and Br^{-}), we use the above form since it works better in simulations and there is no experimental evidence on the distribution of products of this reaction. The original assumption of Jwo and Noyes would give the same result if the hydrogen abstraction reaction from malonic acid by tartronyl radical were used instead of reaction 75. The important point is that a product of the $BrMA^{\bullet}$ hydrolysis should react further to reproduce a malonyl radical.

If the rate constants of these steps are appropriate this sequence can describe the flow experiments, since the malonyl radical that is removed in reaction 61 is replaced in reaction 75. We performed some simulations to test the above assumptions. We used the rate constants of the GTF model for all reactions above, except for k_{38} that proved to be negligibly small in an independent experiment by Försterling and Stuk,[10] thus we set its value to zero. We adjusted the value of k_{84} and we found that the steady state concentration of $MA^{\bullet}$ will be practically independent of [BrMA] in the fast-flow experiments if $k_{84} = 2.5 \times 10^4\ s^{-1}$. We used the same method to determine $[MA^{\bullet}]_{ss}$ as Försterling and Stuk in their simulation, i.e., we started a batch run, and estimated $[MA^{\bullet}]_{ss}$ with $[MA^{\bullet}]$ at 0.22 s. The table below shows the dependence of $[MA^{\bullet}]_{ss}$ on $[BrMA]_0$. Approximate value from Figure 1 of Försterling and Stuk is $[MA^{\bullet}]_{ss} = 3.8 \times 10^{-7}$ M for all $[BrMA]_0$. Smaller k_{84} values decreased $[MA]_{ss}$ as [BrMA] was increased, while larger values caused the opposite effect.

$[BrMA]_0$ (M)	$10^7[MA^{\bullet}]_{ss}$ (M)	calc slope of $\ln([MA^{\bullet}]/[MA^{\bullet}]_{ss})$
0.0	3.75	−0.038
0.05	3.75	−0.072
0.10	3.74	−0.095
0.20	3.74	−0.128
0.45	3.69	−0.178

We also tested the stopped-flow experiments by following the change in $[MA^{\bullet}]$ further than 0.22 s. Since the kinetics shown by the above set of reactions is not clearly first order in $MA^{\bullet}$ when BrMA is present (the reaction is somewhat faster at the beginning) we calculated the average slope between 0.22 and 10.12 s of the $\ln([MA^{\bullet}]/[MA^{\bullet}]_{ss})$ curves as initial slope. These results are also shown in the table above. In agreement with the findings of Försterling and Stuk the initial slope of $\ln[MA^{\bullet}]$ strongly depends on [BrMA]. Approximate slopes for the two extreme situations ($[BrMA]_0 = 0.0$ M and $[BrMA]_0 = 0.45$ M) from Figure 3 of Försterling and Stuk are −0.025 and −0.077 for $[BrMA]_0 = 0$ M and $[BrMA]_0 = 0.45$ M, respectively.

We also checked whether the mechanism suggested above can describe Figure 3 of ref 10 where the rate of reduction of Ce(IV) in various mixtures of MA and BrMA was studied under batch conditions. Our simulation reproduces quantitatively the experiments except for the highest [BrMA] where Försterling and Stuk themselves also suspect experimental artifact. We note here, that the simulated results shown in Figure 3 of ref 10 are probably calculated from the slope of $-\ln([Ce(IV)]/[Ce(IV)]_0)$ not from $+\log([Ce(IV)]/[Ce(IV)]_0)$ as indicated in the text[10] and we also used the first formula to evaluate our own results.

These calculations and the experimental results of Jwo and Noyes[22] suggest, that the hydrolysis of $BrMA^{\bullet}$ should be included in the GTF mechanism, and that then it is possible to interpret semiquantitatively the Försterling–Stuk experiments[10] without excluding the radical transfer from $MA^{\bullet}$ to BrMA.

References and Notes

(1) Belousov, B. P. In *Sb. Ref. Radiat. Med.*; Medgiz: Moscow, 1958, p 145.
(2) Zhabotinsky, A. M. *Biofizika* **1964**, *9*, 306.
(3) Field, R. J.; Körös, E.; Noyes, R. M. *J. Am. Chem. Soc.* **1972**, *94*, 8649.
(4) Györgyi, L.; Turányi, T.; Field, R. J. *J. Phys. Chem.* **1990**, *94*, 7162.
(5) Luo, Y.; Epstein, I. R. *Adv. Chem. Phys.* **1990**, *79*, 269.

(6) Försterling, H.-D.; Noszticzius, Z. *J. Phys. Chem.* **1989**, *93*, 2740.
(7) Försterling, H.-D.; Murányi, S.; Noszticzius, Z. *J. Phys. Chem.* **1990**, *94*, 2915.
(8) Försterling, H.-D.; Murányi, S. *Z. Naturforsch.* **1990**, *45a*, 1259.
(9) Ruoff, P.; Försterling, H.-D.; Györgyi, L.; Noyes, R. M. *J. Phys. Chem.* **1991**, *95*, 9314.
(10) Försterling, H.-D.; Stuk, L. *J. Phys. Chem.* **1991**, *95*, 7320.
(11) Försterling, H.-D.; Stuk, L. *J. Phys. Chem.* **1992**, *96*, 3067.
(12) Field, R. J.; Noyes, R. M. *J. Chem. Phys.* **1974**, *60*, 1877.
(13) Györgyi, L.; Field, R. J. *J. Phys. Chem.* **1991**, *95*, 6594.
(14) Györgyi, L.; Field, R. J. *Nature* **1992**, *355*, 808.
(15) Turányi, T.; Bérces, T.; Vajda, S. *Int. J. Chem. Kinet.* **1989**, *21*, 83.
(16) Turányi, T. *New. J. Chem.* **1990**, *14*, 795.
(17) Turányi, T. *J. Math. Chem.* **1990**, *5*, 203.
(18) Murányi, S.; Försterling, H.-D. *Z. Naturforsch.* **1990**, *45a*, 135.
(19) Ruoff, P.; Noyes, R. M. *J. Phys. Chem.* **1989**, *93*, 7394.
(20) Noszticzius, Z.; Farkas, H.; Schelly, Z. A. *J. Chem. Phys.* **1984**, *80*, 6062.
(21) Noyes, R. M. *J. Chem. Phys.* **1984**, *80*, 6071.
(22) Field, R. J.; Försterling, H.-D. *J. Phys. Chem.* **1985**, *89*, 5400.
(23) Jwo, J.-J.; Noyes, R. M. *J. Am. Chem. Soc.* **1975**, *97*, 5422.
(24) *Rate Constants for Reactions of Aliphatic Carbon-Centered Radicals in Aqueous Solution*; National Bureau of Standards, US Department of Commerce: Washington, DC, October 1982.
(25) Brusa, M. A.; Perissinotti, L. J.; Colussi, A. J. *J. Phys. Chem.* **1985**, *89*, 1572.
(26) Turányi, T. *Comput. Chem.* **1990**, *14*, 253.
(27) Gottwald, B. A.; Wanner, G. *Computing* **1981**, *26*, 355.
(28) Valkó, P.; Vajda, S. *Comput. Chem.* **1984**, *8*, 255.